Article

Evolution of Safety Behavior of High-Power and High-Energy Commercial Li-Ion Cells after Electric Vehicle Aging

Pierre Kuntz [1,2,*], Loïc Lonardoni [2], Sylvie Genies [2], Olivier Raccurt [2] and Philippe Azaïs [2]

1   Entroview, 38400 Saint-Martin-d'Hères, France
2   CEA—Commissariat à l'Energie Atomique et aux Energies Alternatives, LITEN—Laboratoire d'Innovation pour les Technologies des Energies Nouvelles et les Nanomatériaux, DEHT—Département de l'Electricité et de l'Hydrogène pour les Transports, Grenoble Alpes University, 38000 Grenoble, France; loic.lonardoni@cea.fr (L.L.); sylvie.genies@cea.fr (S.G.); olivier.raccurt@cea.fr (O.R.); philippe.azais@cea.fr (P.A.)
*   Correspondence: pierre.kuntz@entroview.com

Abstract: The Li-ion battery is one of the key components in electric car development due to its performance in terms of energy density, power density and cyclability. However, this technology is likely to present safety problems with the appearance of cell thermal runaway, which can cause a car fire in the case of propagation in the battery pack. Today, standards describing safety compliance tests, which are a prerequisite for marketing Li-ion cells, are carried out on fresh cells only. It is therefore important to carry out research into the impact of cell aging on battery safety behavior in order to ensure security throughout the life of the battery, from manufacturing to recycling. In this article, the impact of Li-ion cell aging on safety is studied. Three commercial 18,650 cells with high-power and high-energy designs were aged using a Battery Electric Vehicle (BEV) aging profile in accordance with the International Electrotechnical Commission standard IEC 62-660. Several thermal (Accelerating Rate Calorimetry—ARC) and standardized safety (short-circuit, overcharge) tests were performed on fresh and aged cells. This study highlights the impact of aging on safety by comparing the safety behavior of fresh and aged cells with their aging conditions and the degradation mechanisms involved.

Keywords: Li-ion; battery; aging; degradation mechanisms; abuse test; safety behavior

1. Introduction

Li-ion batteries with graphite-based negative electrodes are now widespread in electric mobility applications thanks to their higher energy density and durability compared to other storage systems. Presently, the main developments in Li-ion batteries concern increasing their energy and power density by developing new positive electrode materials or blending silicon with graphite in the negative electrode. Despite the fact that Li-ion technology has numerous advantages, it has been proven that the Li-ion battery poses a safety risk [1] and is the source of many car fires [2]. Therefore, battery safety assessment is a key issue that must be dealt with in order to continue developing more efficient and durable vehicles, as well as ensuring the user's safety.

The lifetime of Li-ion cells is being continuously improved by innovations, but it is well known that their use can cause degradation mechanisms inside the cell [3,4]. Depending on the storage and cycling conditions, several aging mechanisms can be triggered and induce physical and chemical modifications of the internal components. They can provoke physico-chemical changes, like active material damage [5–11], lithium consumption by SEI growth [5,12–14] and lithium plating [15–19]. These physical and chemical modifications induced by aging first impact cell performance, but can also influence cell safety. Therefore, cell aging conditions have a strong influence on a cell's safety behavior.

One research group has already studied the safety of aged Li-ion cells coupled with *post*-mortem analysis, especially in terms of thermal stability, by performing Accelerating Rate Calorimetry (ARC) tests after cycle aging at 0.5 C and at 0 °C, 5 °C, 25 °C and 45 °C [20]. The tests showed that low-temperature cycle aging reduces cell thermal stability [20,21]. The Li plating phenomenon that takes place on the negative electrode at low temperature ranges is principally responsible for the degradation of safety behavior, because metallic Li reacts exothermally with the electrolyte solvent. On the contrary, high-temperature aging, which induces the degradation mechanism of SEI growth on the negative electrode, does not have a negative impact on the thermal stability of the cell [20,21].

Other studies have also treated the subject of thermal stability but were not always supplemented by *post*-mortem studies. Some studies observed the decrease of thermal stability of cycled cells at low temperatures [22,23], and compared the thermal stability of several cell chemistries, the State Of Health (SOH) and the State of Charge (SOC) [24].

In an accident caused by a Li-ion cell, a temperature increase is always responsible for triggering thermal runaway [25], possibly leading to fire and/or explosion. Electrical solicitations like overcharging and short-circuiting can be responsible for this temperature increase, which is why international safety standards have standardized electrical safety tests (overcharge and short-circuit) to ensure the safety of fresh cells before their sale on the market. To our knowledge, the safety behavior of aged cells during overcharging and short-circuiting has not been discussed in the literature. Studies appear to have focused only on overcharge mechanisms [26] or compared the safety behavior of fresh cells for different chemistries [27].

Our research work has two different parts. The first one concerns the *ante*-mortem analysis of the Li-ion cells studied, the aging of these cells and their *post*-mortem analysis through the identification of the degradation mechanisms involved. A paper on the first part of our work has already been published and bears the title "Identification of Degradation Mechanisms by Post-Mortem Analysis for High Power and High Energy Commercial Li-Ion Cells after Electric Vehicle Aging" [28]. In this first part, the aging process, *ante*-mortem and *post*-mortem analyses (half coin cell at the electrode level, Scanning Electron Microscope (SEM), Energy-Dispersive X-ray (EDX), Glow Discharge-Optical Emission spectrometer (GD-OES), X-Ray Diffraction (XRD), Nuclear Magnetic Resonance (NMR), etc.) have already been performed [28]. This work allows us to understand which main degradation mechanisms occur according to aging conditions, cell chemistry, and design.

The second part of our research work, which is the subject of this article, has the objective of understanding the effects of aging on cell safety. The use of real experimental data from cell aging and aged cell safety tests, coupled with *post*-mortem analysis, highlight the impact on safety of cell internal degradation mechanisms due to aging.

The novelty of this article consists in the understanding on the impact of aging on Li-ion cell safety, through the realization of a large panel of experimental tests: *ante*-mortem study, several aging conditions according to the standards, *post*-mortem study to identify the aging mechanisms involved, and finally abuse and safety tests on fresh and aged cells to highlight the impact of aging on Li-ion cell safety. In addition, this study was carried out on a large amount of cells, divided into three commercial cell references, with 100 units for each reference.

To assess the impact of aging on safety behavior, and not only of thermal behavior, several abuse tests were performed on each fresh and aged cell. Thermal stability was characterized by the ARC test and electrical safety by short-circuiting and overcharging according to the international standard IEC 62-660, part 2 [29]. Data cross-referencing between aging degradation mechanisms [28] and the safety behavior observed enables understanding of the influence of each aging mechanism on the safety of Li-ion cells.

2. Material and Methods

2.1. Samples

The three commercial cells chosen were from SAMSUNG SDI: INR18650-35E (written "35E" afterward), INR18650-32E (written "32E" afterward) and INR18650-30Q (written "30Q" afterward). Each cell of the same reference used in this study comes from the same manufacturer production batch. To ensure that the internal mechanical design, separator and the electrolyte composition of the three samples were similar, the three cells were provided by the same manufacturer.

All the internal components of the fresh and aged cells were analyzed in the first part of our work [28]. The detailed description of the fresh cell chemistry and design, and of the degradation mechanisms occurring inside the aged cells, is described in this paper.

2.2. Aging Tests

Three cell references were investigated using BEV (Battery Electric Vehicle) representative aging at various temperatures (−20 °C, 0 °C, 25 °C, 45 °C), according to the international standard IEC 62-660 part 1 [30], including cycle aging and calendar aging.

Cycle aging was performed at various temperatures (−20 °C, 0 °C, 25 °C, 45 °C). The cycling described in the international standard IEC 62-660 is representative of a typical driving cycle, including a CC-CV charge and a discharge profile with current pulses that simulate braking (charge) and acceleration (discharge) event. SOH assessments using electrical performance measurements were performed every 28 days at 25 °C. The cycling test was stopped once the cell had lost at least 20% of its initial performance in terms of capacity, energy or power density, or after 6 months of cycling.

Calendar aging was achieved at 45 °C, either at constant voltage (CV) at 4.2 V or at 100% SOC in Open Circuit Voltage (OCV, meaning that the voltage was not maintained constantly). The voltage difference between OCV and CV calendar aging was between 0.02 V and 0.1 V maximum after 6 weeks aging. According to the standard, SOH assessments using electrical performance measurements were performed at 25 °C every 6 weeks, and after 18 weeks of storage, the calendar test was stopped.

These electrical measurements were used to trace the evolution of appropriate cell characteristics: capacity, internal resistance and nominal voltage. Each aging procedure was performed on a batch of 15 cells. The periodical electrical performance measurements and cycling test were achieved on a PEC® SBT 05250 test bench (6 V, 50 A).

2.3. Abuse Tests

Thermal stability tests were performed with an ARC EV with Thermal Hazard Technology® equipment. The Heat–Wait–Seek [31] protocol was applied with 5 °C temperature steps, 35 min rest and the detection of the onset temperature (T_{onset}) for a temperature increase of more than 0.02 °C/min. T_{onset} is the temperature at which exothermal reactions start in the cell and the cell starts to heat up by itself.

Overcharging and short-circuiting were carried out on a abuse test bench made specially for this study (shown in Figure 1) at an ambient temperature between 20 °C and 30 °C. According to the standard IEC 62-660 part 2 [29], the short-circuit set-up had a maximum resistance of 5 mΩ and had to be applied for 10 min or until cell failure. Overcharging consisted of applying a current of C (considering the cell capacity at the moment of the test) up to 8.4 V or cell failure. This new abuse test bench allows one to perform up to 6 tests in a row and is fully remote-controllable. The bench was placed in a reinforced box and in a closed room under air suction to ensure the user's safety. The release cylinder works with compressed air and is controlled by an Arduino card. Only one cell can be connected at the same time; this system allows one to connect the chosen cell and change it when the test is finished without entering the room.
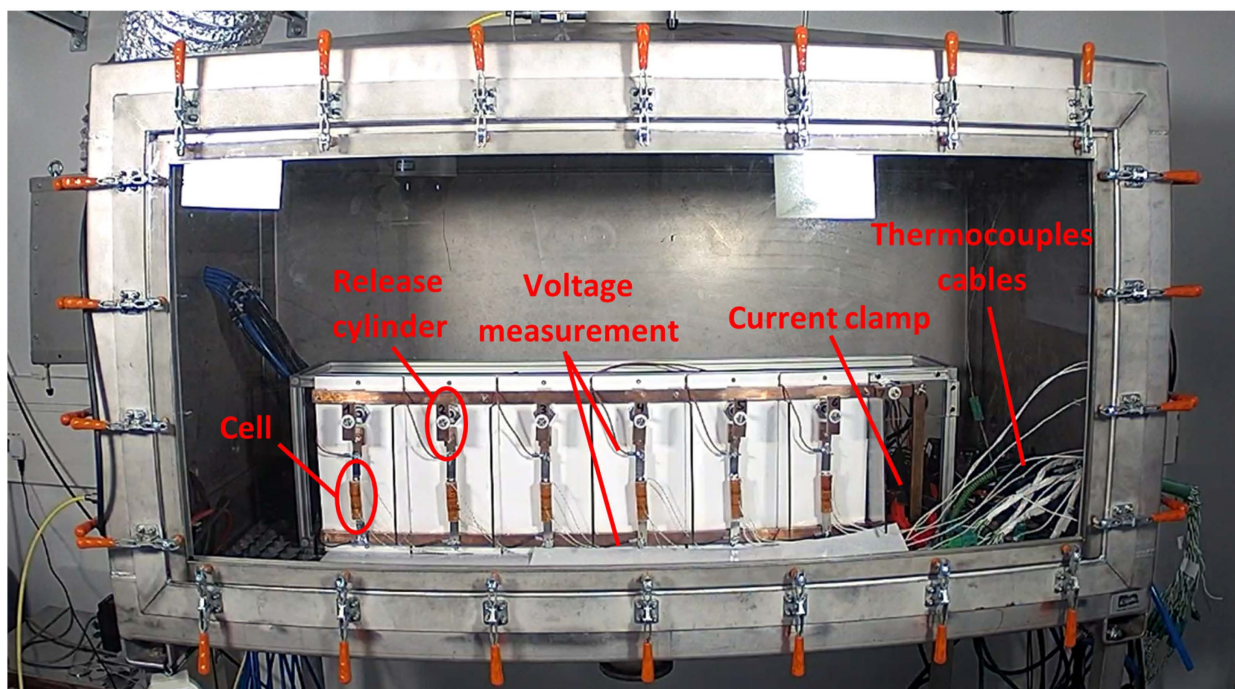
Figure 1. Picture of the abuse test bench specifically developed for this study.

A GM10-2E0 data acquisition unit (Yokogama®) was used for the acquisition of cell voltage, current and temperature. Voltage was measured directly by the unit with a measurement uncertainty of $\leq\pm2.5$ mV. K-type thermocouples were fixed in the middle of each cell using a Kapton tape to ensure the measurement of the surface cell temperature with a measurement uncertainty of $\leq\pm0.3$ °C. The current was measured using an aerometric clamp with measurement uncertainties of $\leq\pm95$ mA for overcharging and $\leq\pm4$ A for short-circuiting.

All the thermal and safety tests were carried out at 100% state of charge (SOC), because it is the worst possible case in terms of safety [24]. Before each test, the cells were charged by a constant current at C/3 until 4.2 V, followed by a constant voltage until C/20. A battery's C-rate is defined by the rate of time in which it takes to charge or discharge; for example, at C/3 it takes 3 h to charge or discharge.

3. Cell Aging and Degradation Mechanism

Before describing a picture of the aging state of sample for each protocol, an overview of the cell materials and design at the initial state is required. One cell of each reference was opened to perform physico-chemical analysis. All the results of the *ante*-mortem analysis are given in the first part of this study, published in a previous paper [28]. Regarding the electrochemical characterization, the three fresh cell batches (100 units) had a very low standard deviation regarding their characteristics in terms of weight, capacity, nominal voltage, internal resistance and energy density.

The chemistry of the three cells showed similarities, but also some differences. 30Q is composed of a blend of NCA ($Li_XNi_yCo_zAl_aO_2$ with $y + z + a = 1$ and $0 < x \leq 1$) + NC ($Li_XNi_wCo_bO_2$ with $w + b = 1$ and $0 < x \leq 1$) on the positive electrode and of a blend of graphite + silicon on the negative electrode. 32E contains only NCA on the positive electrode and only graphite on the negative electrode. 35E also contains only NCA on the positive electrode but a blend of graphite + silicon on the negative electrode. All the detailed chemical compositions of the three cells' electrodes are detailed in our previous paper [28].

The design of the cells was different for the three references: cell 30Q has the thinnest and largest electrodes compared to 35E and 32E. The 30Q cell has a "power" design (i.e.,

"power cells"); indeed, the larger and thinner electrode allows for delivering higher current. On the contrary, the 35E and 32E cells have an "energy" design (i.e., "energy cells"), with thicker and smaller electrodes, which allows optimizing the energy density.

Electrolyte compositions are different but contain similar solvents: ethylene carbonate (EC), dimethyl carbonate (DMC) and fluoroethylene carbonate (FEC). The separator is based on polyethylene (PE) with AlOOH coating on the negative electrode side and is similar for all references.

The *post*-mortem analysis is detailed in the first part of this study published in [28], dedicated to understanding degradation mechanisms after aging. The main conclusions of this previous study are summarized in Table 1.

Table 1. Main degradation mechanisms detected by post-mortem analysis after aging.

Aging Condition		30Q		32E		35E	
		SOH	Degradation Mechanisms	SOH	Degradation Mechanisms	SOH	Degradation Mechanisms
Cycling	−20 °C	85	Li plating ++ Si cracking and disaggregation ++	59	Li plating +++	83	Li plating ++ Si cracking and disaggregation ++
	0 °C	91	Si cracking and disaggregation +	N/A	Li plating ++	70	Si cracking and disaggregation +
	25 °C	76	SEI growth ++	81	SEI growth +	92	SEI growth +
	45 °C	78	SEI growth +++	80	SEI growth ++	86	SEI growth ++
Calendar	45 °C, CV	87	SEI growth +++	80	SEI growth ++	87	SEI growth ++
	45 °C, OCV	91	SEI growth ++	88	SEI growth +	91	SEI growth +

For tests at higher temperatures (25 °C and above), the Solid Electrolyte Interphase (SEI) growth at the negative electrode was a predominant degradation mechanism observed for both types of test (calendar and cycling). This phenomenon is caused by the solvent degradation for calendar aging and salt degradation for cycle aging [28]. During low-temperature cycling (lower than 25 °C), the main aging mechanism identified was the deposition of metallic lithium leading to the formation of a secondary SEI. In addition, silicon can significantly degrade during aging, especially during cycle aging at low temperatures through particle cracking and disaggregation.

The internal design of the cell seemed to have an influence on the aging mechanisms. Energy cells are more sensitive to low-temperature aging, which induces more lithium metal deposition partly due to their higher internal resistance [28]. Power cells, which work well at lower temperatures, are more affected by high temperature with increased growth of SEI due to their larger electrode surface [28].

The nature of the internal components of the cell also has an important influence on the aging mechanisms, since the nature of the electrolyte influences the growth of SEI through solvent degradation and the silicon sometimes present in the negative electrode seems to be a privileged site of degradation.

All the *ante*- and *post*-mortem work carried out enabled the complete analysis of new and aged cells. Thus, the cause-and-effect relationships between the aging conditions and the aging mechanisms were highlighted by this work. For more details about the *ante*- and *post*-mortem work, please refer to our previous paper [28].

Abusive tests were carried out on the three fresh cell references. These results were then compared with those obtained on cells aged according to different aging modes (different temperatures, calendar, cycling) in order to identify the impact of aging on the abusive test behavior.

The 32E cells cycled at 0 °C did not survive the aging subjected by triggering the opening of the current interrupting device—CID, so they could not be tested for the safety study.

4. Results

4.1. Thermal Stability-ARC

Since separator melting (~140 °C) signals the point of no return of thermal runaway, we decided to stay under this point and stop the ARC test at around 100 °C (90 °C for the 30Q, 100 °C for the 35E and 110 °C for the 32E). We focused on the reactions that take place under the separator melting, because they are responsible for the temperature increase leading to the separator melting and therefore to thermal runaway. In the present study, the onset of self-heating was considered in particular because we were interested in the earliest exothermal reactions responsible for cell heating. It is known that the two reactions that occur at the beginning of self-heating are the reaction of inserted and plated lithium if present with solvent [32] after the thermal degradation of the SEI [2,32,33]. Both of those reactions should take place under 90 °C and can be affected by the chemical changes due to aging. Another objective was to not extensively damage the cell for possible further investigations.

Two cells per aging condition were tested in ARC and the results are shown in Figure 2 for T_{onset} and in Figure 3 for the temperature rate. The results are compared to the fresh cell.
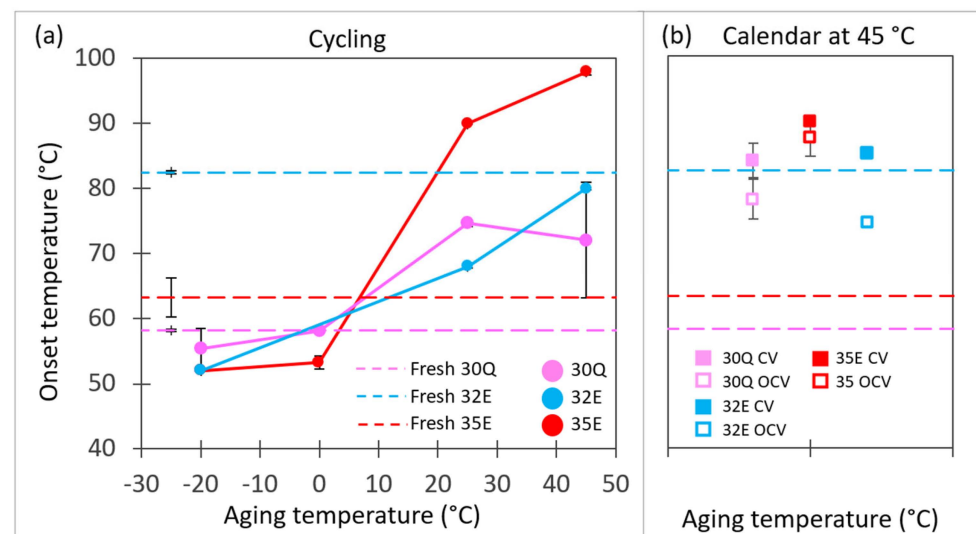

Figure 2. Onset temperature of fresh and aged cells in terms of aging temperature for references 35E, 32E and 30Q, after (**a**) cycle aging and (**b**) calendar aging.

The onset temperature is the beginning of self-heating of the cell due to exothermal reactions during the ARC test. It can be seen that for cells aged at −20 °C and 0 °C, T_{onset} is between 50 °C and 60 °C, and for cells aged at 25 °C and 45 °C T_{onset} is between 65 °C and 100 °C. The change of T_{onset} during aging for the three references T_{onset} is lower after low-temperature cycling than after high-temperature aging (cycling and calendar).

Compared to the fresh cell, two trends can be distinguished. First, the cells containing Si within the negative electrode (30Q and 35E), which has a T_{onset} around 60 °C for the fresh cell, show a decrease of T_{onset} after low-temperature cycling (−20 °C and 0 °C) and, conversely, an increase after high-temperature (45 °C and 25 °C) cycling or calendar storage. Secondly, the cells containing only graphite within the negative electrode (32E), which have a T_{onset} around 80 °C for the fresh cell, show a decrease of T_{onset} after all aging conditions, except after calendar CV storage.
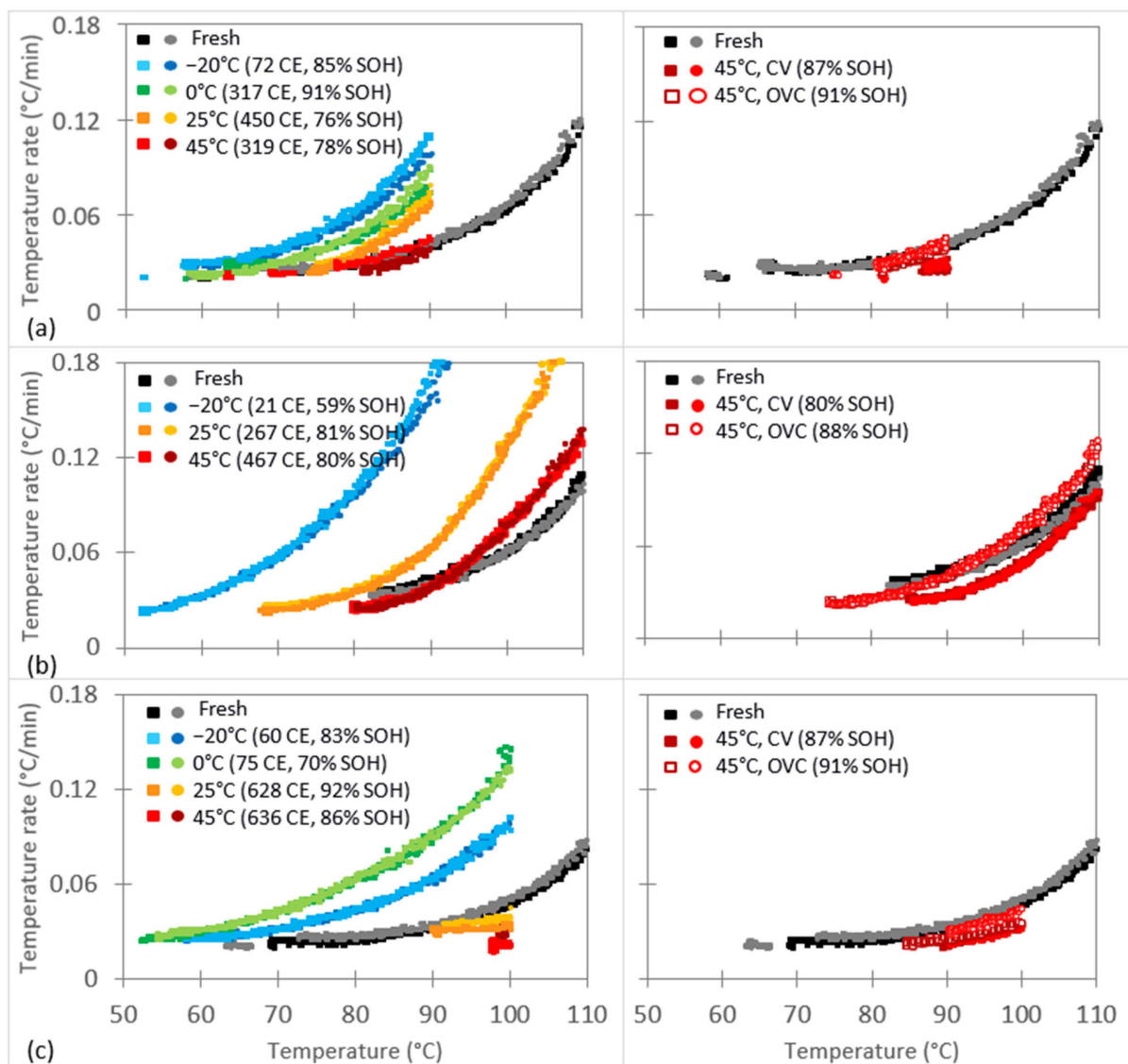
Figure 3. Temperature increase rate during the ARC test of aged and fresh cells for (**a**) 30Q, (**b**) 32E and (**c**) 35E, for 2 cells (square and circle) per aging condition.

The rate of temperature change during the test was also significantly altered by aging. The more the aging was carried out at low temperatures, the faster the temperature rate increased, signifying that the cell was more reactive to self-heating. For example, at 90 °C, the temperature rate increased about 3 times faster for cell 30Q and 6 times faster for cell 32E for a cell aged at −20 °C compared to a cell aged in calendar conditions.

The only exception was for the 35E cell: the temperature of the cells aged at 0 °C increased faster compared to cells aged at −20 °C. However, the behavior at 0 °C can be explained by their lower SOH linked to a more severe damage state (lithium metal deposition and silicon particle degradation). This highlights that the method and the conditions in which the cell is aged had a strong impact on their thermal stability. Systematically, aging at low temperature degraded the thermal stability of the cell.

It is noticeable that for all the cells aged at 45 °C, the temperature rate of the cells was either equivalent to that of the fresh cell or lower for the calendar aging conditions (especially for that set in CV at 4.2 V). This observation reveals that aging at high temperature (especially calendar aging) increased the thermal stability.

Taking into account the *post*-mortem results and the aging effect on thermal stability (T_{onset} and temperature rate), we can assume that the degradation mechanisms of low-

temperature cycling (Li plating [15–19,28] and Si cracking [28,34–36]) degraded the thermal stability of the cell. On the contrary, the degradation mechanisms of high-temperature cycling and storage (SEI growth by salt and solvent degradation) improved the thermal stability of the cell.

4.2. Safety Tests

To evaluate the impact of aging on Li-ion cell safety, short-circuit and overcharge tests were performed on fresh and aged cells. Voltage, current and temperature were tracked during the tests. Particular attention was paid to the temperature because it could show if an accident would occur or not. The results of all the safety tests are described here.

4.2.1. Assessment of the Risk of Short-Circuit

Figure 4 shows the results of short-circuit tests. Data were compared with four parameters: CID opening duration, maximum current, maximum temperature and maximum temperature rate increase. The CID opening duration of a fresh cell is between 10 and 20 s, but after aging it increases to 50 s. CID opening is always longer for aged cells than for new ones. We observed a significant increase of the CID opening duration in particular for energy-designed cells after cycling at low temperature.
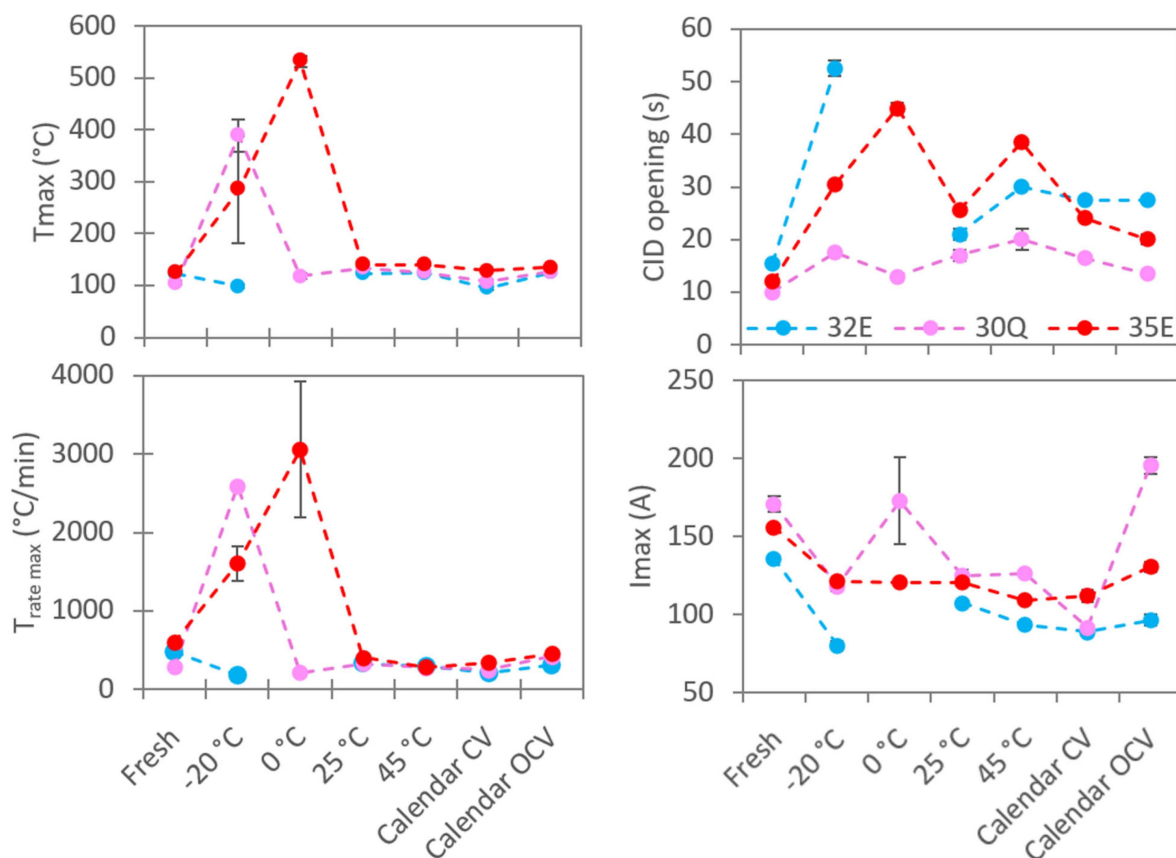

Figure 4. Characteristics of the short-circuit test in terms of CID opening duration, I_{max}, T_{max} and $T_{speed\ max}$ for 30Q, 32E and 35E fresh and aged cells.
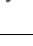
The maximum short-circuit current is generally between 100 A and 200 A. Most of the time, the maximum short-circuit current will decrease after aging in accordance with the increase of cell internal resistance. The short-circuit current also depends on the short-circuit resistance, here between 0 mΩ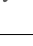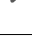 and 5 mΩ, and its variation can explain non-expected values like for 30Q cells after −20 °C and calendar OCV aging.

The maximum temperature reached during the test was between 100 °C and 140 °C for fresh cells. The temperature reached during the short-circuit test was sufficiently high to initiate exothermal reactions inside the cell [2,32,33,37–40], as shown during the ARC test (Figure 3). After aging at 45 °C and 25 °C, the maximum temperature did not change significantly. We could even observe a small decrease of the maximal temperature for the CV calendar-aged cells at 45 °C, confirming that high-temperature aging can be beneficial for cell safety. After aging at low temperature, some cells went into thermal runaway (35E aged at −20 °C and 0 °C and 30Q aged at −20 °C). The maximum temperature reached during short-circuiting was more than 500 °C for 35E cells aged at 0 °C.

The maximum temperature increase rate was between 300 °C/min and 600 °C/min for fresh cells and decreased slightly between 200 °C/min and 500 °C/min for aged cells which did not go into thermal runaway. For the cells that went into thermal runaway, the maximum temperature increase rate could increase up to 3000 °C/min at the cell surface.

Table 2 shows a comparison of the aging degradation mechanisms identified for each aged cell during the *post*-mortem studies and the observation during the short-circuit tests. First, all the fresh cells passed the short-circuit safety test successfully because they did not vent and remained intact. After aging, the CID was no longer efficient enough because venting and explosion of the cells was observed.

Table 2. Short-circuit test results, compared to the SOH and the aging mechanisms identified for each aging condition for cells 30Q, 35E and 32E.

Ref	Fresh	−20 °C	0 °C	25 °C	45 °C	CV	OCV
30Q	✓	85% SOH Li plating Si cracking (explosion)	91% SOH Si cracking (gas and smoke)	76% SOH SEI (gas and smoke)	78% SOH SEI (gas and smoke) (NTR)	87% SOH SEI (NTR)	91% SOH SEI (gas and smoke)
35E	✓	83% SOH Li plating Si cracking (explosion)	70% SOH Si cracking (explosion)	92% SOH SEI (gas and smoke)	86% SOH SEI (gas and smoke)	87% SOH SEI (gas and smoke)	91% SOH SEI (gas and smoke)
32E	✓	59% SOH Li plating (NTR)	Li plating	81% SOH SEI (NTR)	80% SOH SEI (NTR)	80% SOH SEI (NTR)	88% SOH SEI (NTR)

Meaning of symbols: (explosion icon) explosion; (cloud icon) gas and smoke; (green check) NTR.

The 32E cell, unlike the other cells tested, does not contain silicon in the electrode and is not the cause of any negative events. However, we have shown during the post-mortem study of other cell references that silicon was particularly degraded on the surface of the negative electrode. Its considerable volume variations during cycling induced its fragmentation, thus favoring the formation of lithium silicates [28]. The silicon-containing cells exploded after cold aging and often released gases and fumes. It is therefore likely that silicon plays an important role in the safe behavior of the cells, as all the negative events took place in silicon-containing cells, whether or not lithium plating was present.

The energy-type design also appears to be a detrimental factor in terms of safety, as the 35E cell presented more explosions and outgassing than the 30Q cell during the short-circuit tests.

4.2.2. Assessment of the Risk of Overcharge

Figure 5 shows the results of the overcharge tests. Data were compared through three parameters: the final SOC reached at the end of the test, the temperature at the CID opening and the maximum temperature. The final SOC of the overcharge test was between 110% and 130%. The final overcharge SOC can evolve during aging; a significant increase of the final SOC was observed for the energy-designed cell after aging at low temperatures.

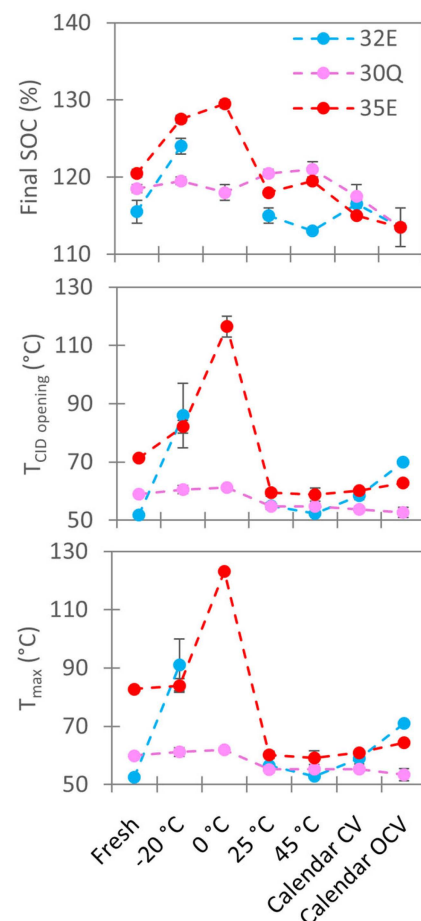This parameter was lower for all the cells after calendar aging, especially for the calendar condition at OCV.

Figure 5. Characteristics of the overcharge test in terms of final SOC, $T_{CID\ opening}$ and T_{max} for 30Q, 32E and 35E fresh and aged cells.

The temperature at the CID opening and the maximum temperature reached were between 50 °C and 120 °C, most often under 70 °C. The temperature at the CID opening was very close to the maximum temperature of the test. It revealed that CID triggers early enough to avoid irrevocable exothermal decomposition reactions. During overcharging, no accident was observed and all cells stayed intact (no venting). However, the cells aged at low temperature had the biggest temperature rise during the test, especially for the energy-designed cells (up to 120 °C), confirming that aging at low temperature decreases cell safety.

5. Discussion

The set of experimental results detailed above highlighted the thermal behavior of fresh and aged cells following standardized protocols and a wide temperature range. An assessment of the risk of the technology throughout its use was thus made possible.

At fresh state, the first two exothermic reactions that cause the cell temperature rise and initiate the thermal runaway are known. They imply SEI decomposition and the direct reaction of inserted lithium with electrolytes, since lithiated graphite is no longer protected by this passivation layer.

The decomposition of the SEI starts at a temperature between 90 °C and 120 °C [2,32,33,37]. The enthalpy of reaction was between 180 and 350 J/g [41]. A representative decomposition reaction considering LiEDC ($(CH_2OCO_2Li)_2$) as the main compound of the SEI is the following:

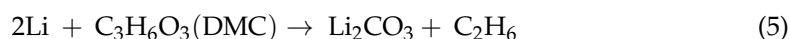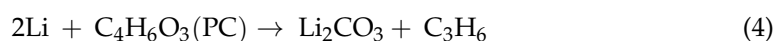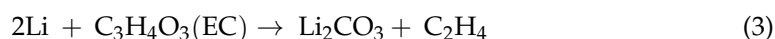$$(CH_2OCO_2Li)_2 \rightarrow Li_2CO_3 + C_2H_4 + CO_2 + \frac{1}{2}O_2 \tag{1}$$
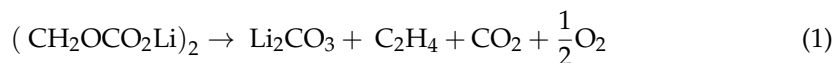
The enthalpy of the direct reaction between organic solvents and lithium inserted within graphite (free of SEI, decomposed beforehand) [32,38] is between 350 and 1714 J/g [41]. The reaction proposed considering only one of the solvents present in the electrolyte (Ethylene carbonate, EC) takes the following form:

$$2Li_xC_6 + C_3H_4O_3(EC) \rightarrow 2Li_{x-1}C_6 + Li_2CO_3 + C_2H_4 \tag{2}$$
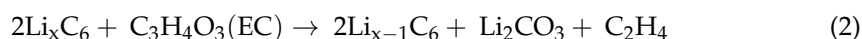
Both the reactions mentioned here can take place simultaneously and generate other reactions when the temperature rises.

After aging, the degradation phenomena generate new exchange surfaces that impact the exothermicity of the cells. One of these phenomena is lithium metal deposition, favored by cycling at low temperatures. Cells aged at very low temperatures (-20 °C), for which we identified the lithium metal deposit on the negative electrode as the main aging mechanism, effectively showed the least thermal stability. When the cell heats up, the lithium metal present on the surface of the negative electrode is directly available to react with the organic solvents in the electrolyte as early as 68 °C [32]. These reactions are exothermic and contribute to the temperature increase of the cell. The presence of electrodeposited lithium metal in the cell is therefore responsible for its greater "reactivity", as the cell heats up earlier and faster. These findings are consistent with the results obtained in the ARC tests with T_{onset} lowering for all cells containing lithium metal. Indeed, whatever the reference studied (30Q, 32E or 35E), the cells in which a lithium metal deposit was observed had a T_{onset} between 50 °C and 60 °C. Exothermic reactions involving lithium metal thus appeared to start as early as 50–60 °C. The following reactions can take place as early as 68 °C according to the literature [32] and have enthalpies between 350 and 1714 J/g [41].

$$2Li + C_3H_4O_3(EC) \rightarrow Li_2CO_3 + C_2H_4 \tag{3}$$

$$2Li + C_4H_6O_3(PC) \rightarrow Li_2CO_3 + C_3H_6 \tag{4}$$

$$2Li + C_3H_6O_3(DMC) \rightarrow Li_2CO_3 + C_2H_6 \tag{5}$$

In some cases, as a function of the amount of plated lithium, when the cell is brought to higher temperatures, the electro-deposited lithium in contact with the electrolyte may oxidize partially or entirely and form a "secondary" SEI [17]. It will no longer be able to react with solvents according to the above-mentioned reactions, or it may be covered with a passivation layer, creating lithium metal islands isolated from the electrolyte and consequently become electrochemically inactive.

SEI growth is the major degradation phenomenon at high temperatures. Cells aged at 45 °C in cycling and calendar conditions are the most thermally stable because when the cell heats up, the first exothermic reaction encountered will be the decomposition of SEI at a temperature between 90 °C and 120 °C [2,32,33,37]. Cells aged at high temperatures are more thermally stable due to a thicker, homogeneous layer of SEI, which explains the start of thermal runaway at higher temperatures than for a fresh cell or for a low-temperature-aged cell.

Regarding the impact of silicon in thermal runaway, it can be noted that the only explosions observed in short-circuit concerned 30Q cells aged at -20 °C and 35E cells aged at -20 °C and 0 °C, i.e., low-temperature-aged cells containing silicon in their negative electrodes. On the other hand, for the 32E cell which did not contain silicon, there was

never any fire, even in the case of aging at $-20\,°C$. Silicon therefore has a significant effect on the thermal stability of the cells. To interpret this result, the mechanical behavior of silicon must be considered. Silicon cycling causes a volume expansion during the lithiation phases and a shrinkage during the delithiation phases [35]. As we observed in post-mortem analysis, these successive volume variations cause cracks and fractionate the particles into smaller and smaller pieces [36,42]. However, it has been shown that the particle size of lithiated silicon has a significant impact on the exothermicity of its degradation between $100\,°C$ and $150\,°C$ [39,40,43]. The disaggregation of lithiated particles of silicon causes a considerable increase in the exchange surface with the electrolyte. This increases the kinetics of the reactions involved and thus the acceleration of cell heating. These reactions start between $100\,°C$ and $150\,°C$ and can therefore lead to additional heating up to reach the separator shrinking temperature, then the triggering of an internal short-circuit, and finally the cell runaway.

Figure 6 shows an illustration of the exothermic reactions present in a low-temperature-aged cell (with lithium metal deposition) containing silicon in the negative electrode. The coupling of lithium metal deposition and silicon degradation is therefore the worst-case scenario in terms of safety. It was in this configuration that we observed cell explosions during the short-circuit tests, the worst stability during the ARC tests and significant heating during overcharging (30Q and 35E cells aged at $-20\,°C$).
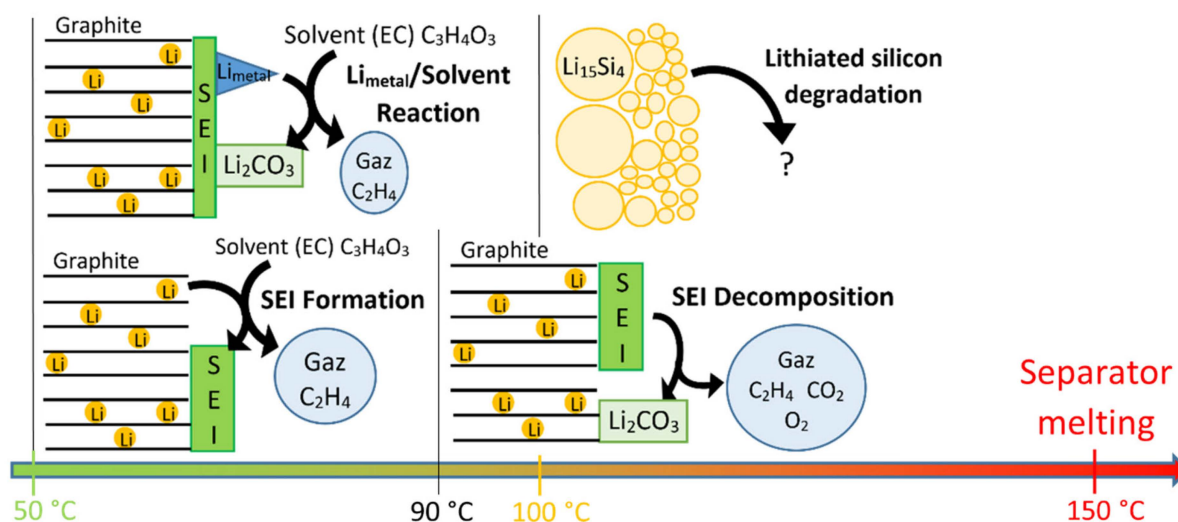

Figure 6. Illustration of the exothermic reactions in a cell containing silicon in the negative electrode and aged at low temperature, with lithium metal deposition.

Finally, this study carried out on energy- and power-designed cells allowed us to assess the impact of cell design on safety. It has been shown that fresh power cells seem to be slightly less stable than fresh energy cells considering their T_{onset} and runaway speed being higher in ARC tests. This observation is still valid after aging at high temperatures ($25\,°C$ and above) in calendar and cycling life. But this must be qualified after ageing at low temperatures. We indeed saw that safety hazards occur more after aging at low temperatures ($-20\,°C$ and $0\,°C$). Energy-type cells age poorly at low temperatures compared to power-type cells. As we saw in our previous study [28], they are more exposed to lithium metal deposition, so their thermal stability degrades more rapidly as the cycling temperature decreases. In addition, energy cells have two major safety disadvantages: a higher internal resistance, which gives them the capacity to heat more easily than a power cell, and a higher energy density (amount of combustible active material), which potentially represents a greater risk in case of accident. The operating temperature range of the battery must therefore be considered when selecting a cell and not only its initial performances to ensure that safety is maintained throughout the aging of the cell. A minimum operating

temperature must be defined to avoid the deposition of metallic lithium for each cell. This minimum temperature is lower for power cells.

6. Conclusions

The influence of aging was correlated with the thermal behavior of cells in the preliminary phase of thermal runaway through three safety tests, i.e., thermal stability, short-circuiting and overcharging. This study showed that the thermal behavior in the runaway phase depends on aging conditions that favor and intensify certain aging mechanisms (SEI growth, Li-plating). Power and energy cell designs must be considered because they do not have the same ability to accept high current, especially at low temperature ranges. Specific experimental devices were set up to perform a large number of tests, which certified that the observed behaviors were clearly repeatable. The exothermic phenomenon involved above 150 °C is the consequence of the separator melting, after which thermal runaway can no longer be controlled. The whole issue of maintaining the safety of this accumulator technology is played out before the separator melts. After aging at room and elevated temperatures, where the main degradation mechanism is the growth of SEI on the surface of the negative electrode, the thermal stability of the cell was improved. Thicker SEI served as a better protective layer by delaying the onset of further exothermic reactions until it decomposed itself. Thermal degradation of SEI is an exothermic phenomenon that can begin as early as 90 °C, but the associated energy is relatively low. After low-temperature aging, in which the main degradation mechanism was the deposition of metallic lithium on the surface of the negative electrode, the thermal stability of the cell was degraded. The electrodeposited lithium in metallic form reacted with solvents as early as about 60 °C. This was the first exothermic reaction that took place with a relatively high reaction enthalpy. It can be delayed if lithium metal is surrounded by a secondary "SEI". The chemistry of the negative active materials also had an influence on the development of its safety behavior. Indeed, we showed that silicon breaks down into smaller particles and that this phenomenon is exacerbated during cold aging. The reactivity of lithiated silicon particles increased significantly as their size decreased. Thus, an additional exothermic reaction took place between 100 and 150 °C in cells containing silicon, and this reaction increased after low-temperature cycling due to the degradation of silicon by fragmentation.

Energy-type cells are more thermally stable in a fresh state, but the significant degradations they undergo during cycling at low temperatures drastically increased the risk of thermal runaway. Power cells, on the other hand, were less stable when fresh, but their better performance in low-temperature cycling made them slightly less exposed to thermal runaway after aging.

The abusive behavior qualification of the Li-ion cells and in particular the corresponding standards must also take aging into account to be able to qualify the safety of the batteries. Finally, these results could contribute towards improving safety standards.

One way of improving the results of this work would be to monitor cell parameters more closely during testing, and achieve greater reproducibility by testing a larger number of cells. However, this is a time-consuming and costly process.

Author Contributions: P.K.: Conceptualization, methodology, experimentation, data curation, writing and supervision. L.L.: experimentation. S.G.: Conceptualization, methodology, experimentation and supervision. O.R. and P.A.: Conceptualization, methodology and supervision. All authors have read and agreed to the published version of the manuscript.

Data Availability Statement: The data are not publicly available.

Conflicts of Interest: The authors declare no conflict of interest.

References

1. Garche, J.; Brandt, K. Safety Considerations with Lithium-Ion Batteries. In *Encyclopedia of Electrochemistry*; Bard, A.J., Ed.; Wiley: Hoboken, NJ, USA, 2020; pp. 1–25. ISBN 978-3-52730-250-5.
2. Lisbona, D.; Snee, T. A Review of Hazards Associated with Primary Lithium and Lithium-Ion Batteries. *Process Saf. Environ. Prot.* **2011**, *89*, 434–442. [CrossRef]
3. Schlasza, C.; Ostertag, P.; Chrenko, D.; Kriesten, R.; Bouquain, D. Review on the Aging Mechanisms in Li-Ion Batteries for Electric Vehicles Based on the FMEA Method. In Proceedings of the 2014 IEEE Transportation Electrification Conference and Expo (ITEC), Dearborn, MI, USA, 15–18 June 2014; pp. 1–6.
4. Waldmann, T.; Iturrondobeitia, A.; Kasper, M.; Ghanbari, N.; Aguesse, F.; Bekaert, E.; Daniel, L.; Genies, S.; Gordon, I.J.; Löble, M.W.; et al. Review—Post-Mortem Analysis of Aged Lithium-Ion Batteries: Disassembly Methodology and Physico-Chemical Analysis Techniques. *J. Electrochem. Soc.* **2016**, *163*, A2149–A2164. [CrossRef]
5. Klett, M.; Eriksson, R.; Groot, J.; Svens, P.; Ciosek Högström, K.; Lindström, R.W.; Berg, H.; Gustafson, T.; Lindbergh, G.; Edström, K. Non-Uniform Aging of Cycled Commercial LiFePO4//Graphite Cylindrical Cells Revealed by Post-Mortem Analysis. *J. Power Sources* **2014**, *257*, 126–137. [CrossRef]
6. Buchberger, I.; Seidlmayer, S.; Pokharel, A.; Piana, M.; Hattendorff, J.; Kudejova, P.; Gilles, R.; Gasteiger, H.A. Aging Analysis of Graphite/LiNi$_{1/3}$Mn$_{1/3}$Co$_{1/3}$O$_2$ Cells Using XRD, PGAA, and AC Impedance. *J. Electrochem. Soc.* **2015**, *162*, A2737–A2746. [CrossRef]
7. Liu, L.; Li, M.; Chu, L.; Jiang, B.; Lin, R.; Zhu, X.; Cao, G. Layered Ternary Metal Oxides: Performance Degradation Mechanisms as Cathodes, and Design Strategies for High-Performance Batteries. *Prog. Mater. Sci.* **2020**, *111*, 100655. [CrossRef]
8. Wohlfahrt-Mehrens, M.; Vogler, C.; Garche, J. Aging Mechanisms of Lithium Cathode Materials. *J. Power Sources* **2004**, *127*, 58–64. [CrossRef]
9. Mukhopadhyay, A.; Sheldon, B.W. Deformation and Stress in Electrode Materials for Li-Ion Batteries. *Prog. Mater. Sci.* **2014**, *63*, 58–116. [CrossRef]
10. Zhou, W.; Hao, F.; Fang, D. The Effects of Elastic Stiffening on the Evolution of the Stress Field within a Spherical Electrode Particle of Lithium-Ion Batteries. *Int. J. Appl. Mech.* **2013**, *05*, 1350040. [CrossRef]
11. Zhou, W. Effects of External Mechanical Loading on Stress Generation during Lithiation in Li-Ion Battery Electrodes. *Electrochim. Acta* **2015**, *185*, 28–33. [CrossRef]
12. Peled, E.; Menkin, S. Review—SEI: Past, Present and Future. *J. Electrochem. Soc.* **2017**, *164*, A1703–A1719. [CrossRef]
13. Grolleau, S.; Delaille, A.; Gualous, H.; Gyan, P.; Revel, R.; Bernard, J.; Redondo-Iglesias, E.; Peter, J. Calendar Aging of Commercial Graphite/LiFePO$_4$ Cell–Predicting Capacity Fade under Time Dependent Storage Conditions. *J. Power Sources* **2014**, *255*, 450–458. [CrossRef]
14. Eddahech, A.; Briat, O.; Vinassa, J.-M. Performance Comparison of Four Lithium–Ion Battery Technologies under Calendar Aging. *Energy* **2015**, *84*, 542–550. [CrossRef]
15. Ecker, M.; Shafiei Sabet, P.; Sauer, D.U. Influence of Operational Condition on Lithium Plating for Commercial Lithium-Ion Batteries–Electrochemical Experiments and Post-Mortem-Analysis. *Appl. Energy* **2017**, *206*, 934–946. [CrossRef]
16. Petzl, M.; Danzer, M.A. Nondestructive Detection, Characterization, and Quantification of Lithium Plating in Commercial Lithium-Ion Batteries. *J. Power Sources* **2014**, *254*, 80–87. [CrossRef]
17. Rangarajan, S.P.; Barsukov, Y.; Mukherjee, P.P. In Operando Signature and Quantification of Lithium Plating. *J. Mater. Chem. A* **2019**, *7*, 20683–20695. [CrossRef]
18. Matadi, B.P.; Geniès, S.; Delaille, A.; Chabrol, C.; de Vito, E.; Bardet, M.; Martin, J.-F.; Daniel, L.; Bultel, Y. Irreversible Capacity Loss of Li-Ion Batteries Cycled at Low Temperature Due to an Untypical Layer Hindering Li Diffusion into Graphite Electrode. *J. Electrochem. Soc.* **2017**, *164*, A2374–A2389. [CrossRef]
19. Senyshyn, A.; Mühlbauer, M.J.; Dolotko, O.; Ehrenberg, H. Low-Temperature Performance of Li-Ion Batteries: The Behavior of Lithiated Graphite. *J. Power Sources* **2015**, *282*, 235–240. [CrossRef]
20. Waldmann, T.; Quinn, J.B.; Richter, K.; Kasper, M.; Tost, A.; Klein, A.; Wohlfahrt-Mehrens, M. Electrochemical, Post-Mortem, and ARC Analysis of Li-Ion Cell Safety in Second-Life Applications. *J. Electrochem. Soc.* **2017**, *164*, A3154–A3162. [CrossRef]
21. Börner, M.; Friesen, A.; Grützke, M.; Stenzel, Y.P.; Brunklaus, G.; Haetge, J.; Nowak, S.; Schappacher, F.M.; Winter, M. Correlation of Aging and Thermal Stability of Commercial 18650-Type Lithium Ion Batteries. *J. Power Sources* **2017**, *342*, 382–392. [CrossRef]
22. Carter, R.; Klein, E.J.; Atkinson, R.W.; Love, C.T. Mechanical Collapse as Primary Degradation Mode in Mandrel-Free 18650 Li-Ion Cells Operated at 0 °C. *J. Power Sources* **2019**, *437*, 226820. [CrossRef]
23. Friesen, A.; Horsthemke, F.; Mönnighoff, X.; Brunklaus, G.; Krafft, R.; Börner, M.; Risthaus, T.; Winter, M.; Schappacher, F.M. Impact of Cycling at Low Temperatures on the Safety Behavior of 18650-Type Lithium Ion Cells: Combined Study of Mechanical and Thermal Abuse Testing Accompanied by Post-Mortem Analysis. *J. Power Sources* **2016**, *334*, 1–11. [CrossRef]
24. Wu, P.; Romberg, J.; Cheng, X.; Hao, W.; Si, H.; Li, H.; Qiu, X. A Study on Thermal Runaway of Commercial Lithium-Ion Cells: Influence of SOC, Cell Chemistry and Ageing Status on Safety Performance. In *Proceedings of the 19th Asia Pacific Automotive Engineering Conference & SAE-China Congress 2017: Selected Papers*; Society of Automotive Engineers (SAE-China), Ed.; Lecture Notes in Electrical Engineering; Springer: Singapore, 2019; Volume 486, pp. 619–627. ISBN 978-981-10-8505-5.
25. Feng, X.; Ouyang, M.; Liu, X.; Lu, L.; Xia, Y.; He, X. Thermal Runaway Mechanism of Lithium Ion Battery for Electric Vehicles: A Review. *Energy Storage Mater.* **2018**, *10*, 246–267. [CrossRef]

26. Belov, D.; Yang, M.-H. Investigation of the Kinetic Mechanism in Overcharge Process for Li-Ion Battery. *Solid State Ion.* **2008**, *179*, 1816–1821. [CrossRef]

27. Brand, M.; Glaser, S.; Geder, J.; Menacher, S.; Obpacher, S.; Jossen, A.; Quinger, D. Electrical Safety of Commercial Li-Ion Cells Based on NMC and NCA Technology Compared to LFP Technology. In Proceedings of the 2013 World Electric Vehicle Symposium and Exhibition (EVS27), Barcelona, Spain, 17–20 November 2013; pp. 1–9.

28. Kuntz, P.; Raccurt, O.; Azaïs, P.; Richter, K.; Waldmann, T.; Wohlfahrt-Mehrens, M.; Bardet, M.; Buzlukov, A.; Genies, S. Identification of Degradation Mechanisms by Post-Mortem Analysis for High Power and High Energy Commercial Li-Ion Cells after Electric Vehicle Aging. *Batteries* **2021**, *7*, 48. [CrossRef]

29. *IEC 62660-2:2018*; Secondary Lithium-Ion Cells for the Propulsion of Electric Road Vehicles-Part 2: Reliability and Abuse Testing. International Electrotechnical Commission: Geneva, Switzerland, 2018.

30. *IEC 62660-1:2018*; Secondary Lithium-Ion Cells for the Propulsion of Electric Road Vehicles-Part 1: Performance Testing. International Electrotechnical Commission: Geneva, Switzerland, 2018.

31. Shelkea, A.V.; Buston, J.E.H.; Gill, J.; Howard, D.; Williams, R.C.E.; Read, E.; Abaza, A.; Cooper, B.; Richards, P.; Wen, J.X. Combined Numerical and Experimental Studies of 21700 Lithium-Ion Battery Thermal Runaway Induced by Different Thermal Abuse. *Int. J. Heat Mass Transf.* **2022**, *194*, 123099. [CrossRef]

32. Wang, Q.; Ping, P.; Zhao, X.; Chu, G.; Sun, J.; Chen, C. Thermal Runaway Caused Fire and Explosion of Lithium Ion Battery. *J. Power Sources* **2012**, *208*, 210–224. [CrossRef]

33. Yang, H.; Bang, H.; Amine, K.; Prakash, J. Investigations of the Exothermic Reactions of Natural Graphite Anode for Li-Ion Batteries during Thermal Runaway. *J. Electrochem. Soc.* **2005**, *152*, A73. [CrossRef]

34. Liu, X.H.; Zhong, L.; Huang, S.; Mao, S.X.; Zhu, T.; Huang, J.Y. Size-Dependent Fracture of Silicon Nanoparticles During Lithiation. *ACS Nano* **2012**, *6*, 1522–1531. [CrossRef]

35. Feng, K.; Li, M.; Liu, W.; Kashkooli, A.G.; Xiao, X.; Cai, M.; Chen, Z. Silicon-Based Anodes for Lithium-Ion Batteries: From Fundamentals to Practical Applications. *Small* **2018**, *14*, 1702737. [CrossRef]

36. Choi, P.; Parimalam, B.S.; Su, L.; Reeja-Jayan, B.; Litster, S. Operando Particle-Scale Characterization of Silicon Anode Degradation during Cycling by Ultrahigh-Resolution X-Ray Microscopy and Computed Tomography. *ACS Appl. Energy Mater.* **2021**, *4*, 1657–1665. [CrossRef]

37. Mikolajczak, C.; Kahn, M.; White, K.; Long, R.T. *Lithium-Ion Batteries Hazard and Use Assessment*; Exponent Failure Analysis Associates, Inc. for Fire Protection Research Foundation: Menlo Park, CA, USA, 2011.

38. von Kolzenberg, L.; Latz, A.; Horstmann, B. Solid–Electrolyte Interphase During Battery Cycling: Theory of Growth Regimes. *ChemSusChem* **2020**, *13*, 3901–3910. [CrossRef] [PubMed]

39. Yoon-Soo, P.; Sung-Man, L. Thermal Stability of Lithiated Silicon Anodes with Electrolyte. *Bull. Korean Chem. Soc.* **2011**, *32*, 145–148. [CrossRef]

40. Profatilova, I.A.; Stock, C.; Schmitz, A.; Passerini, S.; Winter, M. Enhanced Thermal Stability of a Lithiated Nano-Silicon Electrode by Fluoroethylene Carbonate and Vinylene Carbonate. *J. Power Sources* **2013**, *222*, 140–149. [CrossRef]

41. Spotnitz, R.; Franklin, J. Abuse Behavior of High-Power, Lithium-Ion Cells. *J. Power Sources* **2003**, *113*, 81–100. [CrossRef]

42. Kim, M.; Yang, Z.; Bloom, I. Review—The Lithiation/Delithiation Behavior of Si-Based Electrodes: A Connection between Electrochemistry and Mechanics. *J. Electrochem. Soc.* **2021**, *168*, 010523. [CrossRef]

43. Li, C.; Shi, T.; Li, D.; Yoshitake, H.; Wang, H. Dependence of Thermal Stability of Lithiated Si on Particle Size. *J. Power Sources* **2016**, *335*, 38–44. [CrossRef]